Joint oversampled carrier and time-delay synchronization in digital communications with large excess bandwidth ☆

Jordi Vilà-Valls [a,*], Laurent Ros [b], Jean-Marc Brossier [b]

[a] Universitat Politècnica de Catalunya (UPC), Jordi Girona 1-3, 08034 Barcelona, Spain
[b] GIPSA-Lab, Department Image Signal, BP 46 – 38402 Saint Martin d'Hères, France

A B S T R A C T

This paper deals with the joint estimation of the pair dynamical carrier phase/Doppler shift and the time-delay in a digital receiver. We consider a Binary Offset Carrier shaping function as used in satellite positioning, which is a time-limited pulse with a large excess bandwidth, and a Data Aided synchronization scenario, where we have a constant time-delay and a Brownian phase evolution with a linear drift. The proposed study is relative to the use of an oversampled signal model after matched filtering, leading to a colored reception noise and a non-stationary power signal. The contribution of this paper is twofold. First, we derive the Hybrid Cramér–Rao Bound for the joint phase/Doppler estimation problem. Then, we propose a method for the joint time-delay/carrier synchronization, which couples an Extended Kalman Filter and an Expectation-Maximization type algorithm. Our numerical results show the potential gain of using the oversampled signal for carrier synchronization, obtaining better performances than using a classical synchronizer, and good time-delay estimation.

Keywords:
Carrier synchronization
Time-delay synchronization
Hybrid Cramér–Rao bound
Non-linear filtering
Extended Kalman filter
Expectation-maximization
Oversampling
GNSS
BOC

1. Introduction

Synchronization is a fundamental part of Global Navigation Satellite Systems (GNSS). In the synchronization step, we estimate some parameters, such as carrier frequency, carrier phase and time-delay, between each visible satellite and the receiver to estimate the corresponding pseudorange. The synchronizer is coupled with a triangulation algorithm to obtain the receiver's position. In this paper, we focus our attention on the joint carrier phase/frequency offset and time-delay estimation problem in a GNSS-type receiver [2], where we consider a Binary Offset Carrier (BOC) shaping function (as used in new civil GNSS Galileo and the modernized GPS) [3] within a Data-Aided (DA) synchronization scenario.

Many estimation methods for joint carrier and time-delay synchronization have been proposed over the past decades. The time-delay, phase and frequency offset estimation problem is usually solved using Maximum Likelihood (ML) methods.

Historically, the delay and the frequency shift were assumed to be deterministic. In this context, assuming a known transmitted sequence, the optimal way to estimate these two parameters is to search for the maximum of the ambiguity function (delay/Doppler correlation method) [4,5].

For time-varying parameters, the previous method is still useful to provide an initialization to some tracking procedure and the synchronization is then performed as a two-step procedure: coarse and fine estimation, referring to acquisition and tracking, respectively. The acquisition system provides a first estimate of the time-delay and the

☆ Part of this work was presented in conference [1].

* Corresponding author.
E-mail addresses: jordi.vila-valls@upc.edu, jordivilavalls@gmail.com (J. Vilà-Valls).

doi:10.1016/j.sigpro.2011.06.008

Doppler shift and the tracking stage performs a local search for a fine estimation [6]. The tracking is usually based on Phase Locked Loops (PLL)/Delay Locked Loops (DLL) architectures [7,8]. These methods perform correctly with slowly varying phase errors.

For carrier synchronization, an alternative to the classical synchronization methods [8,9] is to reformulate the problem with a dynamic state-space model and to apply Bayesian estimation methods. Several contributions show the use of Kalman-type solutions [10] for carrier synchronization [11–14]. For the joint time-delay and carrier estimation, a solution to solve the ML problem within the state-space formulation is to use a recursive Expectation-Maximization (EM) type algorithm [15]. Recently this approach has been applied to several problems such as channel estimation in OFDM systems [16,17], speech recognition [18] and several parameter estimation and learning problems [19–21].

When having an estimation problem, we need lower bounds on the estimation performance to be used as a benchmark. The family of Cramér–Rao Bounds (CRBs) has been shown to give accurate estimation lower bounds in many scenarios [22]. For time-varying parameter estimation, an analytical expression of a general *online* recursive Bayesian CRB (BCRB) is given by Tichavský et al. [23] and the general formulation for the Hybrid CRB (HCRB), which applies when having both random and deterministic parameters, is derived by Bay et al. [24].

In the literature, most of the lower bounds and the corresponding algorithms assume a white observation noise and a stationary signal.

This contribution, extends and completes the work presented in [25]. We assume a time-varying phase offset modeled as a Brownian motion with a Doppler shift [26] and a constant time-delay over the observation window. We consider an *oversampled* (regarding the symbol time interval) signal model after receiver matched filtering, this implies dealing with a *colored reception noise* and taking into account the non-stationarity of the digital signal power (cyclostationarity when transmitting a random sequence).

Although this scenario is standard in satellite radiolocalization based on a Binary Offset Carrier (BOC) time-limited shaping pulse modulation, there is no theoretical study concerning the performance of the oversampled dynamical phase and frequency offset estimation, and joint time-delay and carrier estimation. In [25], we presented the derivation of a Bayesian CRB for the dynamical phase offset and the EKF that approaches this bound, both presented in a scenario similar to the one treated in this paper.

First, we derive a closed-form expression of the online HCRB for the dynamical phase and frequency offset estimation in the Data Aided (DA) scenario, assuming a Brownian phase evolution with a linear drift (Doppler shift). Secondly, we investigate the use of an EKF based algorithm which can approach this bound (more sophisticated methods such as particle filters or sigma-point Kalman filters are not necessary in this context [25]). We have thus to jointly estimate the colored noise, the dynamical phase and the frequency offset. And finally, we propose an iterative block method to jointly estimate the carrier phase and the time-delay, coupling an EKF-based algorithm and an EM-type solution.

The study allows to measure the potential gain for carrier synchronization provided by the use of the fractionally spaced processing after matched filtering, instead of the symbol time-spaced signal and the good performance obtained with the complete solution.

This paper is organized as follows. Section 2 sets the signal model. Section 3, sets the estimation problem. Section 4, first recalls the HCRB expressions and derives the HCRB for this estimation problem, and then presents the EKF and derives the expressions of the filter in the oversampled phase and frequency offset estimation scenario. Section 5 presents the proposed method for joint time-delay and carrier synchronization. Finally, in Section 6, the numerical results are presented and interpreted. The conclusion is given in Section 7.

Notations: The (k,l)th entry of a matrix $\mathbf{A}$ is denoted $[\mathbf{A}]_{k,l}$. E_x denotes the expectation over x. $\nabla_{\boldsymbol{\theta}}$ and $\Delta^{\boldsymbol{\theta}}_{\boldsymbol{\psi}}$ represent the first and second-order partial derivatives operator, i.e., $\nabla_{\boldsymbol{\theta}} = \left[\partial/\partial\theta_1 \cdots \partial/\partial\theta_K\right]^T$ and $\Delta^{\boldsymbol{\theta}}_{\boldsymbol{\psi}} = \nabla_{\boldsymbol{\psi}}\nabla^T_{\boldsymbol{\theta}}$.

2. Signal model

We propose the signal model for the transmission of a known sequence $\{a_m\}_{m\in\mathbb{Z}}$ over an Additive White Gaussian Noise (AWGN) channel affected by a dynamical carrier phase offset $\theta(t)$ (including the Doppler shift) and a time-delay $\tau(t)$. For an exhaustive derivation see [25].

2.1. Oversampled signal model

2.1.1. Discrete-time general formulation

The received complex baseband signal after matched filtering is

$$y(t) = \left[T_c \sum_m a_m p(t - mT_c - \tau(t)) e^{i\theta(t)} + n(t)\right] * p^*(-t), \tag{1}$$

where T_c,$p(t)$ and $n(t)$ stands for the symbol period, shaping pulse and circular complex Gaussian noise with a known two-sided power spectral density (psd) N_0.

We assume a shaping pulse $p(t)$ with support in $[0,T_c]$, a constant time-delay within the observation window $\tau(t) = \tau$ and a slowly varying phase evolution during a period T_c, which is a usual assumption in satellite communications because the phase variation (due to oscillators phase noise, Doppler shifts, etc.) within one symbol period is small. In this case, the received signal can be written as [25]

$$y(t) = \sum_m a_m g(t - mT - \tau) e^{i\theta(t)} + b(t), \tag{2}$$

where $b(t)$ stands for the filtered colored noise, and $g(t) = p(t) * p^*(-t)$. If we consider a full digital synchronization architecture where the received signal is fractionally spaced at fixed instants $t_k = kT/S$, where S is an integer oversampling factor, we can write the received oversampled signal as

$$y_k = A_k(\tau) e^{i\theta_k} + b'_k, \tag{3}$$

where k refers to t_k instants, so $y_k = y(t_k)$, $\theta_k = \theta(t_k)$ and $b'_k = b(t_k)$, and

$$A_k(\tau) = \sum_m a_m g\left(k\frac{T}{S} - \tau - mT\right). \tag{4}$$

Note that the noise b'_k is colored with variance σ_n^2, where $\sigma_n^2 = N_0 \times g(0)/T_c$ is the variance of the AWGN $n(t)$ measured in the noise equivalent bandwidth of the receiver filter $p^*(-t)$. We can define the symbol index $p = \lfloor k/S \rfloor$, or equivalently, $k = pS + s$ with s the sub-symbol index (i.e., the position inside the symbol interval) and $s = 0, \ldots, S-1$. $\{A_k(\tau)\}_{k\in\mathbb{Z}}$ is a non-stationary power sequence for $S > 1$, even if $\{a_m\}_{m\in\mathbb{Z}}$ is a stationary power symbol sequence ($a_m^2 = 1$).

2.1.2. Discrete-time re-formulation for the noise

The T/S-spaced sequence of noise, $\{b'_k\}_{k\in\mathbb{Z}}$, is defined in the previous section from an analog noise $n(t)$. Our motivation now is to replace this time series by another $\{b_k\}_{k\in\mathbb{Z}}$ with the same statistical properties, but which can be obtained entirely by a discrete-time formulation. This will be useful for the final state-space model formulation. As we did in [25], we can write that the noise samples b'_k have the same statistical properties than samples b_k, which are obtained by a T/S-spaced filtering of the time series n_k:

$$b_k = \sum_{j=0}^{S-1} \Pi_j n_{k-j-1}, \tag{5}$$

where Π_j are the coefficients of the filter which depend on the shaping pulse $p(t)$.

2.2. Parameter evolution model

We consider a constant time-delay τ in the observation window. Concerning the carrier phase, in practice, we have a frequency shift between transmitter's and receiver's carrier oscillator and a Doppler shift due to the relative motion between the satellite and the receiver, so the phase offset is linear with time. We also must consider jitters introduced by oscillators imperfections which can be modeled as a random phase. To take it into account we suppose a Brownian phase offset evolution with a linear drift [26]:

$$\theta_k = \theta_{k-1} + \delta_k + w_k, \tag{6}$$

$$\delta_k = \delta_{k-1}, \tag{7}$$

where $k \geq 2$, w_k is an i.i.d. zero-mean Gaussian noise sequences with known variance σ_w^2/S and δ_k is the unknown constant drift. Here σ_w^2 stands for the variance growth of the phase noise in one symbol interval. We note that the variance of the Gaussian noise is directly related with the rapidity of evolution of the parameter. We note $\mathbf{\Sigma}$ the $N \times N$ covariance matrix of the phase offset evolution, $\boldsymbol{\theta} = [\theta_1 \cdots \theta_N]^T$.

2.3. State-space model

When using an optimal filtering approach a state-space model formulation is needed. As we want to take into account that the observation noise on the output of the matched filter can be colored, we must include it into the state evolution.

The state to be considered includes the phase offset, the drift and the colored noise:

$$\mathbf{x}_k = [\theta_k \;\; \delta_k \;\; b_k \;\; v_k \;\; \cdots \;\; v_{k-S+1}]^T, \tag{8}$$

where $[v_k \;\; v_{k-1} \;\; \cdots \;\; v_{k-S+1}]^T$ is a sliding vector over an i.i.d noise sequence n_k.

We define the state evolution matrix as

$$\mathbf{M}_K = \begin{bmatrix} 1 & 1 & 0 & 0 & \cdots & & 0 \\ 0 & 1 & 0 & 0 & \cdots & & 0 \\ 0 & 0 & 0 & \Pi_0 & & & \Pi_{S-1} \\ 0 & 0 & 0 & 0 & 0 & \cdots & 0 \\ \vdots & \vdots & \vdots & 1 & & & \\ & & & & \ddots & & \\ 0 & 0 & 0 & \cdots & 0 & 1 & 0 \end{bmatrix} \tag{9}$$

and the state noise as $\mathbf{w}_k = [w_k \;\; 0 \;\; 0 \;\; n_k \;\; 0 \;\; \cdots \;\; 0]^T$. From this we have that the state evolution and the observation equation of the state-space model are

$$\mathbf{x}_k = \mathbf{M}_K \mathbf{x}_{k-1} + \mathbf{w}_k, \tag{10}$$

$$y_k = A_k(\tau)\exp(i\theta_k) + b_k. \tag{11}$$

We note that the state equation is linear and the observation equation depends non-linearly on the state. With this formulation we have no observation noise because we have included it in the state.

3. Estimation problem

In this section, we state the estimation problem and we introduce the proposed solution that we will develop in the following sections.

In general, the objective is to jointly estimate the constant time-delay τ and the states (including the carrier phase $\boldsymbol{\theta}$, which has a dynamical evolution, and the constant linear drift δ, which is hidden in the phase evolution) using the received signal $\boldsymbol{y}$. We use the state-space model proposed in Section 2 (Eqs. (10) and (11)) and we consider that the transmitted symbol sequence is known at the receiver (DA synchronization scenario).

In a positioning context, we are interested in the time-delay τ to obtain the pseudorange estimation between each visible satellite and the receiver. In this case, we have to estimate the carrier phase and Doppler shift to obtain a correct estimation of the time-delay. If the received signal is not perturbed by a carrier phase error and a Doppler shift, the time-delay estimation problem can be solved with a simple correlation method. So what complicates the problem is the presence of these parameters.

If τ is known, the states can be inferred using a Kalman filter. Due to the presence of unobserved data (carrier phase and Doppler shift), the ML method to obtain a time-delay estimate cannot be used because the computation of the likelihood function in a closed-form and its maximization w.r.t. τ seems to be an intractable problem. To solve this problem we have to resort to iterative

methods and the natural solution is to use an EM-type solution.

In the following, we first propose a method for phase and frequency shift estimation considering a known delay, and then we use this solution to propose a method for the joint carrier and time-delay estimation.

4. Carrier phase and frequency shift estimation

We consider in this section that we have a good time-delay synchronization (known time-delay), and we focus our attention on the joint carrier phase and frequency shift estimation. First, we compute the HCRB to be used as a benchmark on the estimation error, and then we propose a solution based on a Kalman-type algorithm.

4.1. Hybrid Cramér–Rao bound

When dealing with an estimation problem we aim to know the ultimate accuracy that can be achieved by the estimator. The Cramér–Rao Bounds (CRB) provide a lower bound on the Mean Square Error (MSE) achievable by any unbiased estimator. Depending on the nature of the parameters to be estimated we use different bounds of the CRB family. If the vector of parameters is assumed to be deterministic we use the standard CRB and if the vector of parameters is random and an *a priori* information is available we use the so-called Bayesian CRB [27]. When dealing with both random and deterministic parameters an Hybrid CRB (HCRB) is used [24]. The CRB suited to our problem is the HCRB as we want to estimate the phase offset evolution vector $\boldsymbol{\theta}$ which is a random vector with an *a priori* probability density function (pdf) $p(\boldsymbol{\theta})$ and the linear drift δ which is a deterministic parameter.

In the online synchronization mode, at time k the receiver updates the observation vector $\mathbf{y}=[y_1\cdots y_{k-1}]^T$ including the new observation y_k to obtain the updated vector $\mathbf{y}=[y_1\cdots y_k]^T$ in order to estimate θ_k. In this section we recall the expression of the Hybrid CRB and we present the closed-form expression of the HCRB for an oversampled dynamical phase and frequency offset estimation problem in a Data Aided scenario.

4.1.1. HCRB: background

We have a set of measurements $\mathbf{y}$ and we want to estimate an N-dimensional vector of parameters $\boldsymbol{\mu}=(\boldsymbol{\mu}_r^T\boldsymbol{\mu}_d^T)^T$. We consider the case where the random ($\boldsymbol{\mu}_r$) and the deterministic ($\boldsymbol{\mu}_d$) parts of the vector of parameters can be statistically dependent. We note $\boldsymbol{\mu}_d^*$ the true value of $\boldsymbol{\mu}_d$. The joint probability density of the pair $(\mathbf{y},\boldsymbol{\mu})$ is $p_{\mathbf{y},\boldsymbol{\mu}}(\mathbf{y},\boldsymbol{\mu})$ and the *a priori* pdf of the random part of $\boldsymbol{\mu}$ is $p(\boldsymbol{\mu}_r|\boldsymbol{\mu}_d^*)\neq p(\boldsymbol{\mu}_r)$. If $\hat{\boldsymbol{\mu}}(\mathbf{y})$ is our estimate of $\boldsymbol{\mu}$, the HCRB satisfies the following inequality on the MSE:

$$E_{\mathbf{y},\boldsymbol{\mu}|\boldsymbol{\mu}_d^*}\{[\hat{\boldsymbol{\mu}}(\mathbf{y})-\boldsymbol{\mu}][\hat{\boldsymbol{\mu}}(\mathbf{y})-\boldsymbol{\mu}]^T|\boldsymbol{\mu}_d^*\}\geq\mathbf{H}^{-1}(\boldsymbol{\mu}_d^*), \tag{12}$$

where $\mathbf{H}(\boldsymbol{\mu}_d^*)$ is the so-called Hybrid Information Matrix (HIM) defined as [24]

$$\mathbf{H}(\boldsymbol{\mu}_d^*)=E_{\mathbf{y},\boldsymbol{\mu}_r|\boldsymbol{\mu}_d^*}[-\Delta_{\boldsymbol{\mu}}^{\boldsymbol{\mu}}\log p(\mathbf{y},\boldsymbol{\mu}_r|\boldsymbol{\mu}_d)|\boldsymbol{\mu}_d^*]. \tag{13}$$

Expanding the log-likelihood the HIM can be rewritten as

$$\mathbf{H}(\boldsymbol{\mu}_d^*)=E_{\boldsymbol{\mu}_r|\boldsymbol{\mu}_d^*}[\mathbf{F}(\boldsymbol{\mu}_r,\boldsymbol{\mu}_d^*)]+E_{\boldsymbol{\mu}_r|\boldsymbol{\mu}_d^*}[-\Delta_{\boldsymbol{\mu}}^{\boldsymbol{\mu}}\log p(\boldsymbol{\mu}_r|\boldsymbol{\mu}_d)|\boldsymbol{\mu}_d^*],$$

where $\mathbf{F}(\boldsymbol{\mu}_r,\boldsymbol{\mu}_d^*)$ is the Fisher Information Matrix (FIM) defined as

$$\mathbf{F}(\boldsymbol{\mu}_r,\boldsymbol{\mu}_d^*)=E_{\mathbf{y}|\boldsymbol{\mu}_r,\boldsymbol{\mu}_d^*}[-\Delta_{\boldsymbol{\mu}}^{\boldsymbol{\mu}}\log p(\mathbf{y}|\boldsymbol{\mu}_r,\boldsymbol{\mu}_d)|\boldsymbol{\mu}_d^*]. \tag{14}$$

We can see that $\mathbf{H}(\boldsymbol{\mu}_d^*)=\mathbf{H}^D(\boldsymbol{\mu}_d^*)+\mathbf{H}^P(\boldsymbol{\mu}_d^*)$, where the first term represents the average information about $\boldsymbol{\mu}$ brought by the observations $\mathbf{y}$ and the second term represents the information available from the prior knowledge on $\boldsymbol{\mu}$, i.e., $p(\boldsymbol{\mu}_r|\boldsymbol{\mu}_d)$.

The $N\times N$ HCRB matrix can be written as

$$\mathbf{HCRB}=\{\mathbf{H}(\boldsymbol{\mu}_d^*)\}^{-1}=\{\mathbf{H}^D(\boldsymbol{\mu}_d^*)+\mathbf{H}^P(\boldsymbol{\mu}_d^*)\}^{-1}, \tag{15}$$

where the kth element of the diagonal, $[\mathbf{HCRB}]_{k,k}$ represents the lower bound on the estimation of $[\boldsymbol{\mu}]_k$ from the observations block $\mathbf{y}=[y_1\cdots y_N]$.

4.1.2. HCRB: application to dynamical phase and frequency offset estimation

In this paragraph, a closed-form expression for the HCRB for an online fractionally spaced phase offset and linear drift estimation problem is presented. In the following we drop the dependence of the different matrices on $\boldsymbol{\mu}_d^*=\delta^*$ for easier notation. As we consider a constant drift, for the derivation of the HCRB, we note $\delta_k=\delta$.

We use the model presented in Section 2 (Eqs. (6) and (11)):

$$\theta_k=\theta_{k-1}+\delta+w_k,$$

$$y_k=A_k(\tau)\exp(i\theta_k)+b_k,$$

where, as stated before, b_k is a non-white noise with covariance matrix $\boldsymbol{\Gamma}$. The index k refers to t_k instants and $A_k(\tau)$ are the coefficients specified in Eq. (4) with $\hat{\tau}=\tau$, so we can write that $A_k(\tau)=A_k$.

Comparing this state-space model to the general model presented on the last paragraph, and supposing that we have N available measurements, we identify $\boldsymbol{\mu}_r=\boldsymbol{\theta}=[\theta_1\cdots\theta_N]^T$ and $\boldsymbol{\mu}_d=\delta$. From this the HIM can be rewritten into a $(N+1)\times(N+1)$ block matrix as [24]

$$\mathbf{H}=\begin{pmatrix}\mathbf{H}_{11} & \mathbf{h}_{12}\\ \mathbf{h}_{21} & H_{22}\end{pmatrix}, \tag{16}$$

where

$$\mathbf{H}_{11}=E_{\mathbf{y},\boldsymbol{\theta}|\delta^*}[-\Delta_{\boldsymbol{\theta}}^{\boldsymbol{\theta}}\log p(\mathbf{y}|\boldsymbol{\theta},\delta)|\delta^*]+E_{\boldsymbol{\theta}|\delta^*}[-\Delta_{\boldsymbol{\theta}}^{\boldsymbol{\theta}}\log p(\boldsymbol{\theta}|\delta^*)],$$

$$\mathbf{h}_{12}=\mathbf{h}_{21}^T=E_{\mathbf{y},\boldsymbol{\theta}|\delta^*}[-\Delta_{\boldsymbol{\theta}}^{\delta}\log p(\mathbf{y}|\boldsymbol{\theta},\delta)|\delta^*]+E_{\boldsymbol{\theta}|\delta^*}[-\Delta_{\boldsymbol{\theta}}^{\delta}\log p(\boldsymbol{\theta}|\delta^*)],$$

$$H_{22}=E_{\mathbf{y},\boldsymbol{\theta}|\delta^*}[-\Delta_{\delta}^{\delta}\log p(\mathbf{y}|\boldsymbol{\theta},\delta)|\delta^*]+E_{\boldsymbol{\theta}|\delta^*}[-\Delta_{\delta}^{\delta}\log p(\boldsymbol{\theta}|\delta^*)].$$

So to compute the HIM we need the likelihood function and the *a priori* pdf. From the model we can write the log-likelihood as

$$\log p(\mathbf{y}|\boldsymbol{\theta},\delta^*)=\log\frac{1}{\pi^N|\det(\boldsymbol{\Gamma})|}-[\mathbf{y}-\mathbf{m}]^H\boldsymbol{\Gamma}^{-1}[\mathbf{y}-\mathbf{m}], \tag{17}$$

where $\mathbf{y}$ is the N-dimensional received signal array and $\mathbf{m}$ is the mean vector of $\mathbf{y}$, where the kth component is

$[\mathbf{m}]_k = A_k e^{i\theta_k}$. The *a priori* pdf is

$$\log p(\boldsymbol{\theta}|\delta^*) = \log p(\theta_1) + (N-1)\log\left(\frac{1}{\sqrt{2\pi}\sigma_w}\right) - \sum_{k=2}^{N} \frac{(\theta_k - \theta_{k-1} - \delta^*)^2}{2\sigma_w^2}. \quad (18)$$

Expression of $\mathbf{H}_{11}$: we can write that

$$\mathbf{H}_{11} = \mathbf{H}_{11}^D + \mathbf{H}_{11}^P, \quad (19)$$

where

$$\mathbf{H}_{11}^D = E_{\mathbf{y},\boldsymbol{\theta}|\delta^*}[-\Delta_{\boldsymbol{\theta}}^{\boldsymbol{\theta}} \log p(\mathbf{y}|\boldsymbol{\theta},\delta)|\delta^*],$$

$$\mathbf{H}_{11}^P = E_{\boldsymbol{\theta}|\delta^*}[-\Delta_{\boldsymbol{\theta}}^{\boldsymbol{\theta}} \log p(\boldsymbol{\theta}|\delta^*)].$$

The first term can be computed from Eq. (17). We note $\Lambda(\boldsymbol{\theta}) = \log p(\mathbf{y}|\boldsymbol{\theta},\delta)$. The first derivative of $\Lambda(\boldsymbol{\theta})$ with respect to the lth phase parameter is

$$\begin{aligned}\frac{\partial \Lambda(\boldsymbol{\theta})}{\partial \theta_l} &= \frac{\partial}{\partial \theta_l}\{-[\mathbf{y}-\mathbf{m}]^H \boldsymbol{\Gamma}^{-1}[\mathbf{y}-\mathbf{m}]\} \\ &= \left\{\frac{\partial \mathbf{m}^H}{\partial \theta_l}\boldsymbol{\Gamma}^{-1}[\mathbf{y}-\mathbf{m}] + [\mathbf{y}-\mathbf{m}]^H\boldsymbol{\Gamma}^{-1}\frac{\partial \mathbf{m}}{\partial \theta_l}\right\} \\ &= 2\Re\left\{\frac{\partial \mathbf{m}^H}{\partial \theta_l}\boldsymbol{\Gamma}^{-1}[\mathbf{y}-\mathbf{m}]\right\}. \end{aligned} \quad (20)$$

If we compute now the derivative with respect to the kth phase parameter we have that

$$\frac{\partial^2 \Lambda(\boldsymbol{\theta})}{\partial \theta_k \partial \theta_l} = 2\Re\left\{\frac{\partial^2 \mathbf{m}^H}{\partial \theta_k\, \partial \theta_l}\boldsymbol{\Gamma}^{-1}[\mathbf{y}-\mathbf{m}] - \frac{\partial \mathbf{m}^H}{\partial \theta_l}\boldsymbol{\Gamma}^{-1}\frac{\partial \mathbf{m}}{\partial \theta_k}\right\}. \quad (21)$$

The (k,l)th element of the matrix $\mathbf{H}_{11}^D$ is

$$\begin{aligned}[\mathbf{H}_{11}^D]_{k,l} &= E_{\boldsymbol{\theta}|\delta^*}\left\{E_{\mathbf{y}|\boldsymbol{\theta},\delta^*}\left\{-\frac{\partial^2 \Lambda(\boldsymbol{\theta})}{\partial \theta_k \partial \theta_l}\right\}\right\} \\ &= E_{\boldsymbol{\theta}|\delta^*}\left\{2\Re\left\{\frac{\partial \mathbf{m}^H}{\partial \theta_l}\boldsymbol{\Gamma}^{-1}\frac{\partial \mathbf{m}}{\partial \theta_k}\right\}\right\}. \end{aligned}$$

We note that

$$\frac{\partial \mathbf{m}^H}{\partial \theta_l} = [0,\ldots,0,-iA_l^* e^{-i\theta_l},0,\ldots,0], \quad (22)$$

$$\frac{\partial \mathbf{m}}{\partial \theta_k} = [0,\ldots,0,iA_k e^{i\theta_k},0,\ldots,0]^T, \quad (23)$$

with the non-null values on the lth and kth position, respectively, and so the coefficients can be written as

$$\begin{aligned}[\mathbf{H}_{11}^D]_{k,l} &= E_{\boldsymbol{\theta}|\delta^*}\{2\Re\{A_l^* A_k \cdot [\boldsymbol{\Gamma}^{-1}]_{k,l} e^{j(\theta_k-\theta_l)}\}\} \\ &= 2\Re\{A_l^* A_k \cdot [\boldsymbol{\Gamma}^{-1}]_{k,l} E_{\boldsymbol{\theta}|\delta^*}\{e^{j(\theta_k-\theta_l)}\}\}. \end{aligned}$$

We can write that

$$E_{\boldsymbol{\theta}}\{e^{i(\theta_k-\theta_l)}\} = E_{\boldsymbol{\theta}}\{e^{i(\mathbf{u}_{kl}^T\boldsymbol{\theta})}\} = \phi(\mathbf{u}_{kl}), \quad (24)$$

where $\mathbf{u}_{kl}^T = [0,\ldots,0,(+1),0,\ldots,0,(-1),0,\ldots,0]$, $+1$ in the kth position and -1 in the lth position of the array, $\phi(\cdot)$ is the characteristic function of a Gaussian random variable $\boldsymbol{\theta}$:

$$\begin{aligned}\phi(\mathbf{u}_{kl}) &= \exp\{-\tfrac{1}{2}\mathbf{u}_{kl}^T\boldsymbol{\Sigma}^{-1}\mathbf{u}_{kl}\} \\ &= \exp\{-\tfrac{1}{2}([\boldsymbol{\Sigma}^{-1}]_{k,k} + [\boldsymbol{\Sigma}^{-1}]_{l,l} - 2[\boldsymbol{\Sigma}^{-1}]_{k,l})\}, \end{aligned} \quad (25)$$

with $\boldsymbol{\Sigma}$ the covariance matrix of the phase evolution $\boldsymbol{\theta}$. Finally

$$[\mathbf{H}_{11}^D]_{k,l} = 2\Re\{A_l^* A_k [\boldsymbol{\Gamma}^{-1}]_{k,l} e^{\Psi}\}, \quad (26)$$

where

$$\Psi = \{-\tfrac{1}{2}([\boldsymbol{\Sigma}^{-1}]_{k,k} + [\boldsymbol{\Sigma}^{-1}]_{l,l} - 2[\boldsymbol{\Sigma}^{-1}]_{k,l})\}. \quad (27)$$

We note that the elements $[\boldsymbol{\Sigma}^{-1}]_{k,k}$ are proportional to S/σ_w^2, so for small values of σ_w^2 ($\sigma_w^2 < 0.1$) we have that $e^{\Psi} \sim 0$ except when $k=l$ where $e^{\Psi} = 1$. As an example representing the worst of the cases, when we set $S=1$, $\sigma_w^2 = 0.1$, $k=1$ and $l=N$, $e^{\Psi} = 4.54 \times 10^{-5}$.
As we assume that the phase variation is small over the symbol interval (hypothesis done in Section 2), we can consider that $\mathbf{H}^D$ is a diagonal matrix with

$$[\mathbf{H}_{11}^D]_{k,k} = 2|A_k|^2 [\boldsymbol{\Gamma}^{-1}]_{k,k}. \quad (28)$$

In the following we compute the second term of Eq. (19). From the state evolution equation (6) and assuming that the initial phase θ_1 does not depend on δ, we have that

$$p(\boldsymbol{\theta}|\delta^*) = p(\theta_1)\Pi_{k=2}^N p(\theta_k|\theta_{k-1},\delta^*) \quad (29)$$

and due to this expansion we can rewrite the expression as

$$\Delta_{\boldsymbol{\theta}}^{\boldsymbol{\theta}} \ln p(\boldsymbol{\theta},\delta^*) = \Delta_{\boldsymbol{\theta}}^{\boldsymbol{\theta}} \ln p(\theta_1) + \sum_{k=1}^{N} \Delta_{\boldsymbol{\theta}}^{\boldsymbol{\theta}} \ln p(\theta_k|\theta_{k-1},\delta^*). \quad (30)$$

The first term in Eq. (30) is a matrix with only one non-zero element, namely, the entry (1,1) which is equal to

$$[\Delta_{\boldsymbol{\theta}}^{\boldsymbol{\theta}} \ln p(\theta_1)]_{1,1} = \frac{\partial^2 \ln p(\theta_1)}{\partial \theta_1^2}. \quad (31)$$

The other terms are matrices with only four non-zero elements, namely, the entries $(k-1,k-1)$, $(k-1,k)$, $(k,k-1)$ and (k,k). Due to the Gaussian nature of the noise, one finds

$$[\Delta_{\boldsymbol{\theta}}^{\boldsymbol{\theta}} \ln p(\theta_k|\theta_{k-1},\boldsymbol{\delta}^*)]_{k,k} = \frac{-S}{\sigma_w^2}, \quad (32)$$

$$[\Delta_{\boldsymbol{\theta}}^{\boldsymbol{\theta}} \ln p(\theta_k|\theta_{k-1},\boldsymbol{\delta}^*)]_{k,k-1} = \frac{S}{\sigma_w^2}. \quad (33)$$

The values for $(k-1,k-1)$ and $(k-1,k)$ are, respectively, the same that for (k,k) and $(k-1,k)$. Assuming that $E_{\theta_1}[\Delta_{\boldsymbol{\theta}}^{\boldsymbol{\theta}} \ln p(\theta_1)] = 0$ that corresponds to the case of non-informative prior about θ_1, we obtain that

$$\begin{aligned}\mathbf{H}_{11}^P &= E_{\boldsymbol{\theta}|\delta^*}[-\Delta_{\boldsymbol{\theta}}^{\boldsymbol{\theta}} \log p(\boldsymbol{\theta}|\delta^*)] \\ &= \frac{1}{\sigma_w^2/S}\begin{pmatrix} 1 & -1 & 0 & \cdots & 0 \\ -1 & 2 & -1 & \ddots & \vdots \\ 0 & \ddots & \ddots & \ddots & 0 \\ \vdots & & -1 & 2 & -1 \\ 0 & \cdots & 0 & -1 & 1 \end{pmatrix}. \end{aligned} \quad (34)$$

Expression of $\mathbf{h}_{12}$: the log-likelihood (Eq. (17)) does not depend on δ so the first term of $\mathbf{h}_{12}$ is null, so

$$\mathbf{h}_{12} = E_{\boldsymbol{\theta}|\delta^*}[-\Delta_{\boldsymbol{\theta}}^{\delta} \log p(\boldsymbol{\theta}|\delta^*)].$$

From the state model we have that

$$\mathbf{h}_{12} = \left[\frac{S}{\sigma_w^2} \;\; \mathbf{0}_{1\times N-2} \;\; -\frac{S}{\sigma_w^2}\right]^T.$$

Expression of H_{22}: as the log-likelihood does not depend on δ and using Eq. (18) we have that

$$\begin{aligned} H_{22} &= E_{\boldsymbol{\theta}|\delta^*}[-\Delta_\delta^\delta \log p(\boldsymbol{\theta}|\delta^*)] \\ &= E_{\boldsymbol{\theta}|\delta^*}\left[-\frac{\partial^2}{\partial\delta^2}\log p(\boldsymbol{\theta}|\delta^*)\right] = \frac{S(N-1)}{\sigma_w^2}. \end{aligned}$$

Remarks: As we analyze the estimation problem in a DA scenario the bound depends on the transmitted sequence **a**. In this paper, we suppose the transmission of a known sequence to analyze the performance of the proposed algorithm and the bound. We note that the HCRB is computed for a specific known sequence. The bound depends on the sequence, the oversampling factor S and the position s inside the symbol interval of the current transmitted symbol (index M):

$$HCRB_\theta(\mathbf{a},S,s) = [\mathbf{H}^{-1}(\mathbf{a})]_{N,N}, \tag{35}$$

$$HCRB_\delta(\mathbf{a},S,s) = [\mathbf{H}^{-1}(\mathbf{a})]_{N+1,N+1}, \tag{36}$$

with $N = (M-1)*S+1+s$.

4.2. Extended Kalman filter for carrier phase and frequency shift estimation

In the sequel, we recall the notation and the basics of the Kalman filter and we derive the EKF [28] for the oversampled carrier phase and frequency offset estimation.

4.2.1. Kalman background

We consider that we have a system described by the following state-space equations pair

$$\begin{aligned} \mathbf{x}_{k+1} &= f_k(\mathbf{x}_k) + \mathbf{w}_k, \\ \mathbf{y}_k &= g_k(\mathbf{x}_k) + \mathbf{v}_k, \end{aligned} \tag{37}$$

where $\mathbf{x}_k$ is the state vector, $\mathbf{w}_k$ is a zero-mean white noise with covariance matrix $\mathbf{Q}_k$, $\mathbf{y}_k$ is the observation vector at time k which is a partial and noisy observation of the state $\mathbf{x}_k$ and $\mathbf{v}_k$ is the observation noise with covariance matrix $\mathbf{R}_k$. Noises $\mathbf{w}_k$ and $\mathbf{v}_k$ are supposed to be uncorrelated. The functions $f_k(\cdot)$ and $g_k(\cdot)$ can be non-linear in a general case.

We note $\widehat{\mathbf{x}}_{k|m}$, the estimation of $\mathbf{x}_k$ from the observations up to time m, $\tilde{\mathbf{x}}_{k|m} = \mathbf{x}_k - \widehat{\mathbf{x}}_{k|m}$, the estimation error and $\mathbf{P}_{k|m} = E(\tilde{\mathbf{x}}_{k|m}\tilde{\mathbf{x}}_{k|m}^T)$, the covariance matrix of the estimation error. For Gaussian, linear state models, the KF gives the best Mean Square Error (MSE) estimation of the state $\mathbf{x}_k$ from observations up to time k. For non-linear problems, the EKF gives a sub-optimal estimator $\widehat{\mathbf{x}}_{k|k}$ in a recursive way: the main idea is to linearize the state-space equations at each iteration in order to transform the filtering problem into a usual Kalman one.

4.2.2. EKF: the algorithm

To derive the EKF, we need to compute $\partial f_k(\mathbf{x}_k)/\partial\mathbf{x}_k$ and $\partial g_k(\mathbf{x}_k)/\partial\mathbf{x}_k$.

In the state-space model for oversampled phase estimation presented in Section 2 (Eqs. (10) and (11)), the state equation is linear, hence $\partial f_k(\mathbf{x}_k)/\partial\mathbf{x}_k = \mathbf{M}_K$. The state noise covariance $\mathbf{Q}$ is independent from k and has only two non-zero elements: $[\mathbf{Q}]_{1,1} = \sigma_w^2/S$ and $[\mathbf{Q}]_{3,3} = \sigma_n^2$. Because we introduced the colored noise b_k into the state, there is no observation noise and the covariance matrix $\mathbf{R}$ is null. The observation equation is non-linear versus the state, we have to apply a linearization:

$$\mathbf{g} = \frac{\partial g_k(\widehat{\mathbf{x}}_{k|k-1})}{\partial\mathbf{x}_k} = [iA_k(\tau)e^{i\widehat{\theta}_{k|k-1}} \;\; 0 \;\; 1 \;\; 0 \;\; \cdots \;\; 0]^T. \tag{38}$$

Finally, the EKF expressions for the oversampled algorithm are

$$\begin{cases} \mathbf{P}_{k|k-1} = \mathbf{M}_K\mathbf{P}_{k-1|k-1}\mathbf{M}_K^H + \mathbf{Q}, \\ \widehat{\mathbf{x}}_{k|k-1} = \mathbf{M}_K\widehat{\mathbf{x}}_{k-1|k-1}, \\ \mathbf{K}_k = \mathbf{P}_{k|k-1}\mathbf{g}^H\{\mathbf{g}\mathbf{P}_{k|k-1}\mathbf{g}^H\}^{-1}, \\ \mathbf{P}_{k|k} = [\mathbf{I} - \mathbf{K}_k\mathbf{g}]\mathbf{P}_{k|k-1}, \\ \widehat{\mathbf{x}}_{k|k} = \widehat{\mathbf{x}}_{k|k-1} + \mathbf{K}_k[\mathbf{y}_k - A_k(\tau)e^{i\widehat{\theta}_{k|k-1}} - \widehat{b}_{k|k-1}], \end{cases} \tag{39}$$

where $\mathbf{I}$ is the identity matrix with appropriate dimension.

5. Joint time-delay and carrier synchronization method

In this section, we propose an iterative block method for joint time-delay and carrier synchronization. The method is inspired by the EM algorithm [15], which is an iterative method to find the ML estimate of given desired parameter in the presence of unobserved data or nuisance parameters. The idea behind the algorithm is to augment the observed data with latent data, which can be either missing data or parameter values.

Our method is then based on an iterative optimization of a cost function to find the time-delay (desired parameter in the EM formulation), coupled with the Kalman-type solution proposed in Section 4 for the estimation of the carrier phase and the Doppler shift (nuisance parameters in the EM solution).

5.1. The proposed method

The main goal is to write a function that only depends on the time-delay, $\mathcal{L}(\tau)$, that we will optimize iteratively. The starting point is the joint pdf:

$$p(\mathbf{y},\boldsymbol{\theta};\tau) = p(\mathbf{y}|\boldsymbol{\theta};\tau)p(\boldsymbol{\theta};\tau). \tag{40}$$

From the state-space model, the *a priori* density $p(\boldsymbol{\theta})$ is

$$p(\boldsymbol{\theta}) = p(\theta_1)\prod_{k=2}^{N} p(\theta_k|\theta_{k-1}), \tag{41}$$

where $p(\theta_k|\theta_{k-1})$ are Gaussian densities with mean θ_{k-1} and variance σ_w^2, so we can write

$$p(\boldsymbol{\theta}) = \left(\frac{1}{\sqrt{2\pi}\sigma_w}\right)^{N-1}\exp\left\{-\frac{1}{2\sigma_w^2}\sum_{k=2}^{N}(\theta_k-\theta_{k-1})^2\right\}. \tag{42}$$

In a DA context, the likelihood function w.r.t. τ is

$$p(\mathbf{y}|\mathbf{a},\boldsymbol{\theta};\tau) = \mathcal{N}(\mathbf{y};\mathbf{m}(\boldsymbol{\theta},\tau),\boldsymbol{\Gamma}),$$

where $\mathbf{m}(\boldsymbol{\theta},\tau)$ is the mean vector with $[\mathbf{m}(\boldsymbol{\theta},\tau)]_k = A_k(\tau)e^{i\theta_k}$ and $\boldsymbol{\Gamma}$ is the covariance matrix of the observation noise. The product of these densities is

$$p(\mathbf{y}|\boldsymbol{\theta};\tau)p(\boldsymbol{\theta}) = \left(\frac{1}{\sqrt{2\pi}\sigma_w}\right)^{N-1}\frac{1}{\pi^N|\det(\boldsymbol{\Gamma})|} \times\exp\left\{-[\mathbf{y}-\mathbf{m}(\boldsymbol{\theta},\tau)]^H\boldsymbol{\Gamma}^{-1}[\mathbf{y}-\mathbf{m}(\boldsymbol{\theta},\tau)]-\frac{1}{2\sigma_w^2}\sum_{k=2}^{N}(\theta_k-\theta_{k-1})^2\right\} \tag{43}$$

and so

$$\ln p(\mathbf{y},\boldsymbol{\theta};\tau) = C(\sigma_w^2,\boldsymbol{\Gamma})-[\mathbf{y}-\mathbf{m}(\boldsymbol{\theta},\tau)]^H\boldsymbol{\Gamma}^{-1}[\mathbf{y}-\mathbf{m}(\boldsymbol{\theta},\tau)] -\frac{1}{2\sigma_w^2}\sum_{k=2}^{N}(\theta_k-\theta_{k-1})^2. \tag{44}$$

We assume that at the jth iteration of the method, the time-delay estimated at the previous step $\hat{\tau}^{(j-1)}$ is available. As we want to obtain a function that only depends on τ, and optimize it with respect to this parameter, all the terms in the log-density that do not depend on the time-delay can be omitted. So we consider the function

$$\begin{aligned}\mathcal{F}(\boldsymbol{\theta},\tau) &= -[\mathbf{y}-\mathbf{m}(\boldsymbol{\theta},\tau)]^H\boldsymbol{\Gamma}^{-1}[\mathbf{y}-\mathbf{m}(\boldsymbol{\theta},\tau)]\\ &= -\mathbf{y}^H\boldsymbol{\Gamma}^{-1}\mathbf{y}+\mathbf{y}^H\boldsymbol{\Gamma}^{-1}\mathbf{m}(\boldsymbol{\theta},\tau)\\ &\quad+\mathbf{m}(\boldsymbol{\theta},\tau)^H\boldsymbol{\Gamma}^{-1}\mathbf{y}-\mathbf{m}(\boldsymbol{\theta},\tau)^H\boldsymbol{\Gamma}^{-1}\mathbf{m}(\boldsymbol{\theta},\tau).\end{aligned} \tag{45}$$

At the jth iteration, we obtain a function that only depends on the time-delay τ by taking the (conditional) expectation of $\mathcal{F}(\boldsymbol{\theta},\tau)$ with respect to the carrier phase $\boldsymbol{\theta}$ (given the knowledge of $\mathbf{y},\mathbf{a},\hat{\tau}^{(j-1)}$),

$$\begin{aligned}\mathcal{L}^{(j)}(\tau) &= \mathbb{E}_{\boldsymbol{\theta}|\mathbf{y},\mathbf{a},\hat{\tau}^{(j-1)}}[\mathcal{F}(\boldsymbol{\theta},\tau)]\\ &= -\mathbf{y}^H\boldsymbol{\Gamma}^{-1}\mathbf{y}+\mathbf{y}^H\boldsymbol{\Gamma}^{-1}\mathbb{E}_{\boldsymbol{\theta}|\mathbf{y},\mathbf{a},\hat{\tau}^{(j-1)}}[\mathbf{m}(\boldsymbol{\theta},\tau)]\\ &\quad+\mathbb{E}_{\boldsymbol{\theta}|\mathbf{y},\mathbf{a},\hat{\tau}^{(j-1)}}[\mathbf{m}(\boldsymbol{\theta},\tau)^H]\boldsymbol{\Gamma}^{-1}\mathbf{y}\\ &\quad-\mathbb{E}_{\boldsymbol{\theta}|\mathbf{y},\mathbf{a},\hat{\tau}^{(j-1)}}[\mathbf{m}(\boldsymbol{\theta},\tau)^H\boldsymbol{\Gamma}^{-1}\mathbf{m}(\boldsymbol{\theta},\tau)],\end{aligned} \tag{46}$$

where the terms $\mathbb{E}_{\boldsymbol{\theta}|\mathbf{y},\mathbf{a},\hat{\tau}^{(j-1)}}[\mathbf{m}(\boldsymbol{\theta},\tau)]$ and $\mathbb{E}_{\boldsymbol{\theta}|\mathbf{y},\mathbf{a},\hat{\tau}^{(j-1)}}[\mathbf{m}(\boldsymbol{\theta},\tau)^H\boldsymbol{\Gamma}^{-1}\mathbf{m}(\boldsymbol{\theta},\tau)]$ only depend on the carrier phase. If we consider that we have an estimate of these two terms, we can estimate the time-delay at the current iteration from the previous time-delay estimate $\hat{\tau}^{(j-1)}$, by maximizing the cost function $\mathcal{L}^{(j)}(\tau)$ w.r.t. τ

$$\hat{\tau}^{(j)} = \arg\max_{\tau}\mathcal{L}(\tau)^{(j)}. \tag{47}$$

The method iterates the optimization until the convergence of the sequence $(\ldots,\hat{\tau}^{(j)},\hat{\tau}^{(j+1)},\ldots)$.

Using the characteristic function of a Gaussian density, we can write that

$$[\mathbb{E}_{\boldsymbol{\theta}|\mathbf{y},\mathbf{a},\tau^{(j-1)}}[\mathbf{m}(\boldsymbol{\theta},\tau)]]_k = A_k(\tau)\mathbb{E}_{\boldsymbol{\theta}|\mathbf{y},\mathbf{a},\hat{\tau}^{(j-1)}}[e^{i\theta_k}] = A_k(\tau)e^{i\widehat{\theta}_k}e^{-(1/2)\sigma^2_{\hat{\theta}_k}}$$

where the estimate of the mean $\widehat{\theta}_k^{(j)}$ and the variance $\sigma^2_{\hat{\theta}_k}(j)$ can be obtained from a Kalman-type solution as presented in Section 4. The remaining term can be written as

$$\mathbb{E}_{\boldsymbol{\theta}|\mathbf{y},\mathbf{a},\tau^{(j-1)}}\left[\frac{1}{\sigma_n^2}\mathbf{m}(\boldsymbol{\theta},\tau)^H\mathbf{m}(\boldsymbol{\theta},\tau)\right] = \frac{1}{\sigma_n^2}\sum_k|A_k(\tau)|^2.$$

So the cost function to be maximized is

$$\mathcal{L}^{(j)}(\tau) = -\left\{\mathbf{y}^H\mathbf{y}-\mathbf{y}^H\mathrm{diag}(\boldsymbol{d}(\tau))\mathbf{t}(\widehat{\boldsymbol{\theta}}^{(j)}) -\mathbf{t}^H(\widehat{\boldsymbol{\theta}}^{(j)})\mathrm{diag}(\boldsymbol{d}(\tau)^*)\mathbf{y}+\sum_k|A_k(\tau)|^2\right\}$$

$$\mathcal{L}^{(j)}(\tau) = -\|\mathbf{y}-\mathrm{diag}(\boldsymbol{d}(\tau))\mathbf{t}(\widehat{\boldsymbol{\theta}}^{(j)})\|^2, \tag{48}$$

where $[\mathbf{d}(\tau)]_k = A_k(\tau)$ and $[\mathbf{t}(\widehat{\boldsymbol{\theta}})]_k = (e^{\widehat{i\theta}_k^{(j)}}e^{-(1/2)\sigma^{2(j)}_{\hat{\theta}_k}})$. Finally, the proposed method is based on the following optimization:

$$\hat{\tau}^{(j)} = \arg\max_{\tau}\left\{2\Re(\mathbf{y}^H\mathrm{diag}(\boldsymbol{d}(\tau))\mathbf{t}(\widehat{\boldsymbol{\theta}}^{(j)}))-\sum_k|A_k(\tau)|^2\right\}. \tag{49}$$

The iterative block method is sketched in Algorithm 1 and a scheme is given in Fig. 1.

Algorithm 1. Joint time-delay, carrier phase and Doppler shift estimation method.

Require: Block of N observations $y_{p:p+N-1}$, process and measurement noise statistics.
1: **initialization**
2: **for** i=1 to convergence of the algorithm **do**
3: **for** j=p to p+N-1 **do**
4: Estimation of θ_j and δ using the Extended Kalman filter in Eq. (39).
5: **end for**
6: Time-delay estimation $\hat{\tau}^{(i)}$ from Eq. (49).
7: **end for**

To summarize: we have an iterative approximation of the ML solution for the estimation of the time-delay τ (block method) where we embed a Kalman-type solution to obtain the carrier phase and Doppler shift estimates (operating sample-wise).

This method resembles a classic DA ML method for the estimation of the time-delay after previous estimation and compensation of the carrier phase and Doppler shift. Indeed the cost function in (48) can be regarded as kind of distance between the observations and the expected noiseless signal after a carrier phase correction.

The advantage of our method is that it works iteratively to estimate the carrier phase/Doppler shift and the time-delay. Each operation can then be used to enhance the estimation performance of the other one giving rise to an iterative technique. Actually this intuitive idea is the basis of all the turbo methods for joint parameters estimation. The EM-type formulation used here is a way to arrive to the iterative technique more rigorously [16].

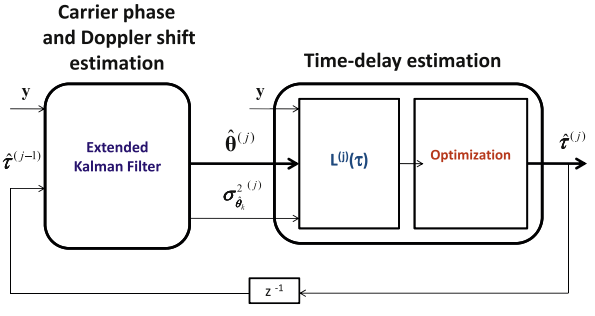

Fig. 1. Block scheme of the joint estimation method.

5.2. Computational complexity

The purpose of this section is to determine the implementation complexity in terms of the number of multiplications needed for our algorithm. The iterative method proposed is composed of two stages: carrier phase and Doppler shift estimation using an extended Kalman filter and time-delay estimation with the maximization of a cost function.

Concerning the first stage, the complexity of the *time update* step of the Kalman filter (state prediction and covariance of the prediction error) is $(n_x^2+2n_x^3)$ and the complexity of the *measurement update* step (Kalman gain, state update and covariance of the measurement update error) is $(2n_x+5n_x^2)$, where $n_x=\dim(\mathbf{x}_k)$ is the state dimension (n_x=4, 5 and 7 for S=1,2 and 4, respectively, see Eq. (8)). So the Kalman stage complexity is $\mathcal{O}(Nn_x^3)$, where N is the block size. The computational complexity of the optimization stage (Eq. (49)) is $(3N)$, therefore, the bottleneck of the algorithm is the first stage and the overall computational complexity of our algorithm is at each iteration of the EM algorithm $\mathcal{O}(Nn_x^3)$.

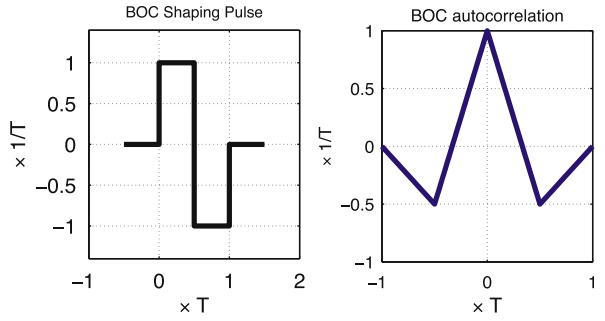

Fig. 2. BOC shaping function $\Pi(t)$ and its autocorrelation $g(t)$.

6. Computer simulations

In this section we show the behavior of the proposed method by considering different scenarios. To assess the method's performance we assume the transmission over an AWGN channel of a M-sequence of length 511 bits generated using a Linear Feedback Shift Register (LFSR) with characteristic polynomial $[1021]_8$ (octal representation). We consider three oversampling factors (S=1,2 and 4) and a BOC shaping pulse (see Fig. 2). We fix the drift to $\delta=0.2$.

First we present the performance obtained with the Extended Kalman Filter for joint carrier phase and frequency shift estimation considering two scenarios:

- perfect time-delay synchronization,
- estimated time-delay.

In this case, we plot the Root Mean Square Error (RMSE), obtained over 250 independent Monte Carlo runs, versus the Signal to Noise Ratio (SNR). The SNR corresponds to the Carrier to Noise Ratio (C/N) at the input of the receiver. In our case, as shaping pulse and symbols a_k are normalized (i.e., $\sigma_a^2=1; g(0)=1$) this ratio is simply $C/N=1/\sigma_n^2$. The performances obtained are compared with the HCRB. We compute the bound and the RMSE for the T-spaced symbol reference points for S=1,2,4 (see [25] for the comparison of the estimation using T-spaced

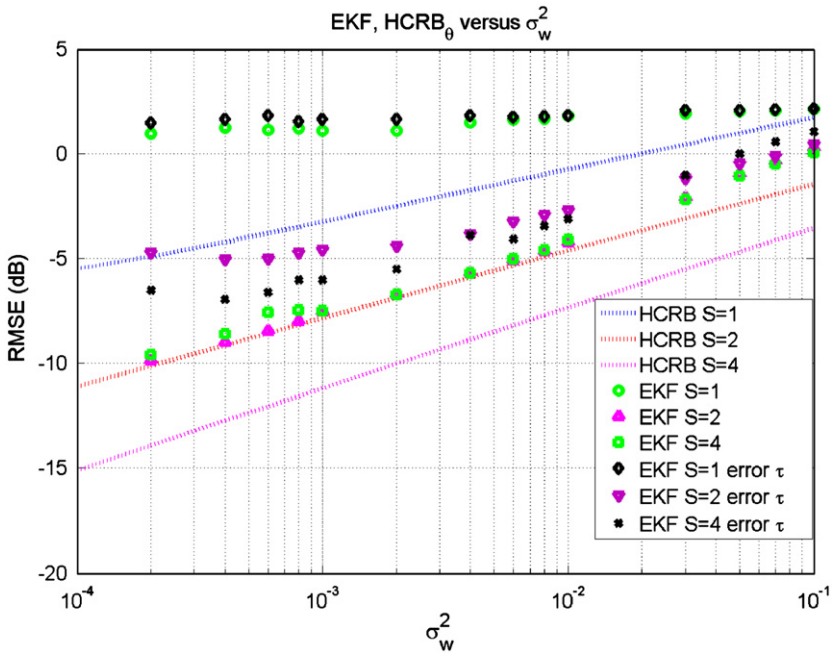

Fig. 3. HCRB and RMSE obtained with the EKF, for the carrier phase estimation, versus the phase noise variance for three different oversampling factors S=1, 2 and 4, and a fixed low SNR= −20 dB. We consider two scenarios: perfect time-delay synchronization and an error on the delay estimation $\hat{\tau}-\tau=T_c/8$.

symbol reference points and T-spaced symbol mid-points and more scenarios). We note that we compared our method with the standard carrier synchronization Fitz's method [9] but this completely fails in our scenarios, which is clear because this method assumes a deterministic phase distortion.

In Fig. 3 we analyze the HCRB and the EKF behavior for a fixed SNR versus phase noise variance. We present a scenario with a really low SNR (as used in satellite based poisioning), SNR $=-20$ dB. We can see that using 1 point per symbol ($S=1$) the performances on the estimation are far from the theoretical bound. This is because the CRB does not give a good lower bound in the large error regions. In counterpart, with $S=2$ and 4 we can measure the gain given by the oversampling and the good performance of the algorithm. The gain obtained with the oversampling is greater at small σ_w^2. We also plot on the same figure the performances obtained with an error on the time-delay estimation ($\hat{\tau}-\tau=T_c/8$), We can see that the performances are worse than those obtained with

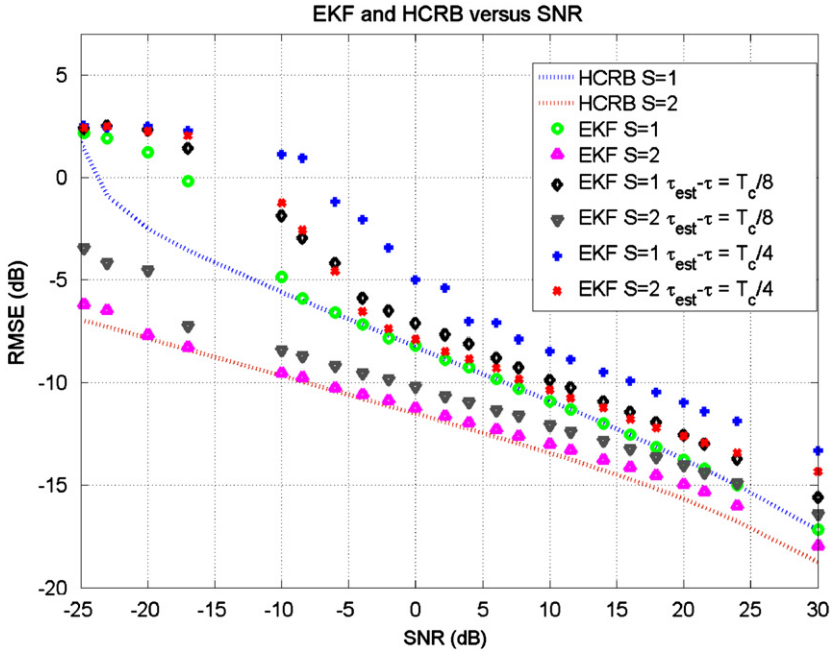

Fig. 4. HCRB and RMSE obtained with the EKF, for the carrier phase estimation, versus the SNR for three different oversampling factors $S=1$, 2 and 4, and a fixed phase noise variance $\sigma_w^2=0.001$. We consider three scenarios: perfect time-delay synchronization, an error on the delay estimation $\hat{\tau}-\tau=T_c/8$ and an error $\hat{\tau}-\tau=T_c/4$.

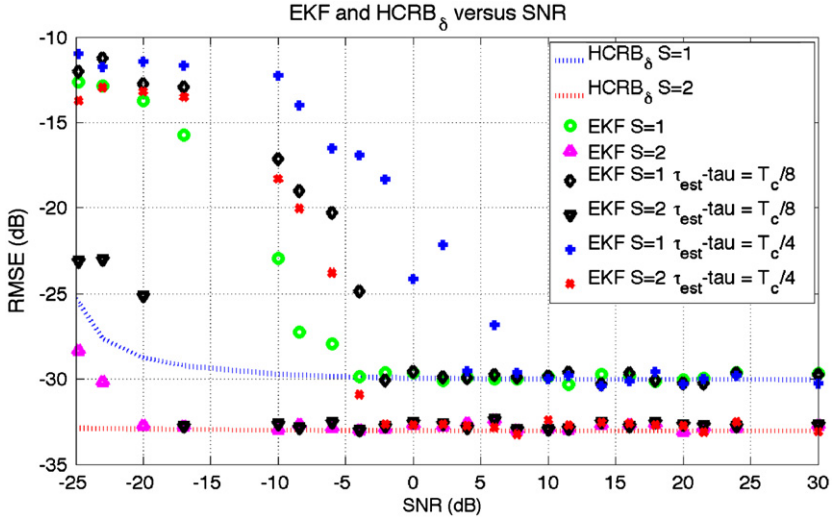

Fig. 5. HCRB and RMSE obtained with the EKF, for the estimation of the Doppler shift, versus the SNR for three different oversampling factors $S=1$, 2 and 4, and a fixed phase noise variance $\sigma_w^2=0.001$. We consider three scenarios: perfect time-delay synchronization, an error on the delay estimation $\hat{\tau}-\tau=T_c/8$ and an error $\hat{\tau}-\tau=T_c/4$.

a perfect time-delay synchronization but still acceptable with $S=2$ and $S=4$.

Fig. 4 superimposes, versus the SNR, the online HCRB and the RMSE obtained with the EKF. We have a phase with a moderate variation, $\sigma_w^2 = 0.001$ rad^2. We assume three different scenarios: a perfect time-delay synchronization, an error on the delay estimation of $\hat{\tau}-\tau = T_c/8$ and a greater error $\hat{\tau}-\tau = T_c/4$. We do not plot the case $S=4$ because the results are the same as for $S=2$. Let us consider the perfect synchronization case: for $S=1$ the performance of the EKF fits the HCRB except for really low SNR where the performance is degraded (and the CRB is not a good benchmark in large error regions). For $S=2$ the EKF performance is slightly looser than the bound. The gain increases with the oversampling factor S and the interest of oversampling becomes clear at low SNR, what is the usual case in satellite based poisioning. The gain due to oversampling decreases as the SNR increases. The performance gain between oversampling factors S decreases proportionally to the phase noise variance σ_w^2. For the estimated (error) time-delay scenarios we note that the performances obtained are a little bit worse than with the perfect synchronization but are still acceptable.

Fig. 5 superimposes, versus the SNR, the RMSE obtained with the EKF and the online HCRB for the Doppler shift estimation. We consider a phase noise variance $\sigma_w^2 = 0.001$, three oversampling factors $S=1,2,4$ and a fixed block size $N=511$ (we note that the performance on the estimation of the drift depends on the block size N because the parameter to be estimated has a constant value). We note that the performances increase when increasing S and the convergence to the lower bound depends on the error on the time-delay estimation and the oversampling factor. But in all the cases we obtain a good estimation of the Doppler shift.

After the analysis of the carrier phase and Doppler shift estimation we consider the joint time-delay and carrier synchronization estimation problem (the main concern of the paper).

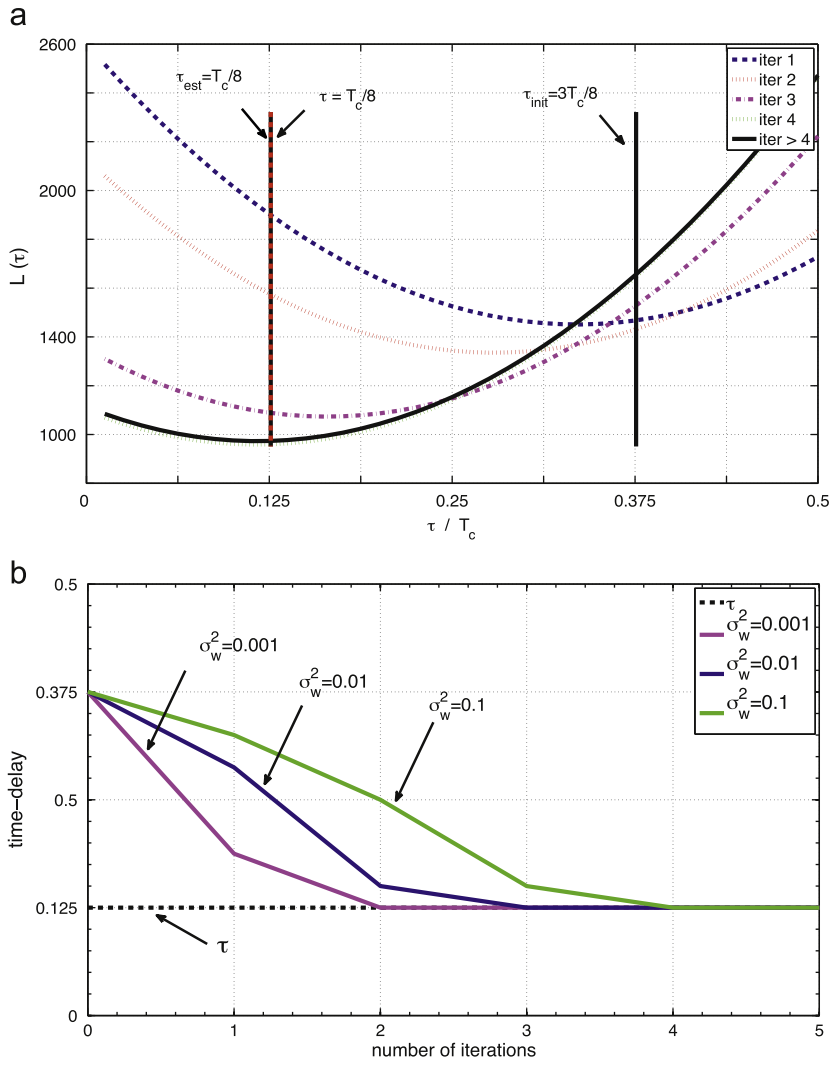

Fig. 6. SNR=0 dB, $\tau = T_c/8$ and $\tau_{init} = 3T_c/8$. (a) Values of the function to be optimized $\mathcal{L}(\tau)$ in different iterations for a fast varying phase evolution, $\sigma_w^2 = 0.1$. (b) Convergence of the algorithm for three phase noise variances: $\sigma_w^2 = 0.001$, $\sigma_w^2 = 0.01$ and $\sigma_w^2 = 0.1$.

The convergence and performance of the algorithm mainly depend on the process and measurement noises affecting the system and on the estimation of the carrier phase provided by the first stage. We first consider the joint estimation in a scenario with a SNR = 0 dB where the algorithm almost always converges to the true value (see the table at the end of the section). In Fig. 6(a), we plot the function to be optimized $\mathcal{L}(\tau)$ for different iterations of a single realization of the algorithm (with a really fast varying phase offset with variance $\sigma_w^2 = 0.1$) and in Fig. 6(b) we show the convergence of the algorithm for different carrier phase evolutions ($\sigma_w^2 = 0.001, 0.01$ and 0.1). In both cases the true time-delay is $\tau = T_c/8$ and the algorithm is initialized at $\tau_{init} = 3T_c/8$.

We note that the speed of convergence depends on the phase and observation noises, and that stronger the noises

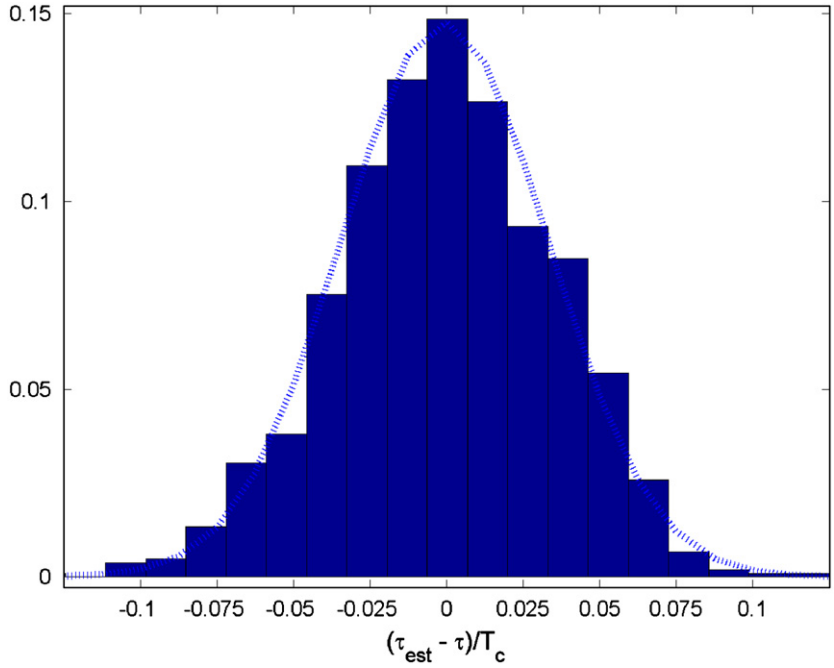

Fig. 7. e-pdf and Gaussian fitted distribution (dotted line) for the time-delay estimation error. SNR = −10 dB and $\sigma_w^2 = 0.001$.

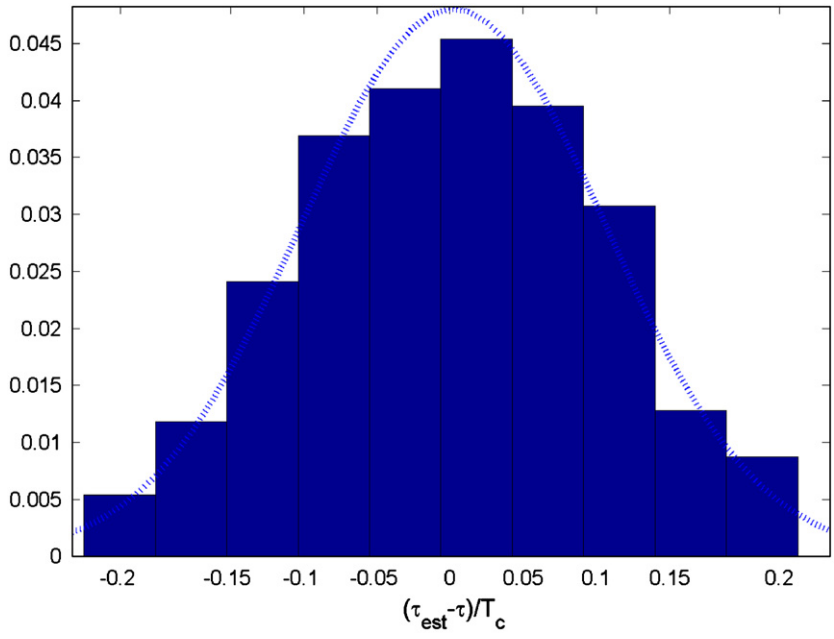

Fig. 8. e-pdf and Gaussian fitted distribution (dotted line) for the time-delay estimation error. SNR = −20 dB and $\sigma_w^2 = 0.001$.

lower the speed of convergence. Indirectly we can see that the good performance of the algorithm directly depends on the carrier estimation stage performance. We also note that in this scenario (where the measurement noise is not really strong) we obtain a good time-delay estimation with few iteration, so the performances obtained with the proposed method are encouraging. But we have to analyze the behavior of the algorithm for lower values of SNR (down to -20 dB) and the error associated on the estimation procedure.

On the following we plot the empirical probability density function (e-pdf) of the error on the time-delay estimation for different scenarios, which is computed over 1000 independent Monte Carlo runs. As a reference we fit a Gaussian distribution to the same sample data sets. In Fig. 7, we plot the e-pdf and the fitted Gaussian distribution for a phase evolution with $\sigma_w^2 = 0.001$ and a SNR$=-10$ dB. In Fig. 8, we consider the same scenario but with a really low SNR$=-20$ dB. In both cases we use a block size $N=511$, the true time-delay is $\tau = T_c/4$ and the algorithm is initialized at $\tau_{init} = T_c/2$.

We can see that the Gaussian distribution fits correctly with the e-pdf of the time-delay estimation error. In the following table we show the empirical mean and standard deviation computed from the error sample set considering different signal to noise ratios and block sizes:

SNR (dB)	Mean	Std. dev.	N
-20	$T_c/4$	$0.1T_c$	511
-10	$T_c/4$	$0.033T_c$	511
0	$T_c/4$	$0.01T_c$	511
10	$T_c/4$	$2\times10^{-3}T_c$	511
0	$T_c/4$	$0.0134T_c$	300
0	$T_c/4$	$0.0167T_c$	200
0	$T_c/4$	$0.0227T_c$	100
0	$T_c/4$	$0.0309T_c$	50

We note that the mean is always equal to the true time-delay but the standard deviation is three times greater in the case SNR$=-20$ dB compared with the SNR$=-10$ dB case. Even in these conditions (really low SNR scenarios) the performances obtained are still acceptable. The error on the other two cases, SNR$=0$ and 10 dB, are really weak and the algorithm converges to the true value almost always. We also give the sample mean and standard deviation with different block sizes (for SNR$=0$ dB). We can see that smaller the block size greater the variance of the estimation error.

7. Conclusion

In usual transmission systems, the roll-off is between 0% and 100%, however, in the context of satellite positioning systems, like GPS and GALILEO, time-limited shaping pulse are used and the Nyquist–Shannon sampling theorem does not apply. These special conditions let us hope a significant receiver synchronization performance improvement when the received signal is oversampled (using more than one sample per symbol).

In this paper, we study the gain due to an oversampling of the received signal for the problem of dynamical carrier phase tracking, and we propose a method for joint carrier and time-delay synchronization. Assuming that the data are known at the receiver, we derive the Hybrid Cramér–Rao Bound for carrier estimation, and we couple a Kalman-based DA algorithm and an EM-type method for joint carrier and time-delay estimation in such an oversampled scenario.

This study shows several improvements when a fractionally spaced method for phase and frequency offset estimation is used. The estimation MSE decreases as the oversampling factor S increases and the interest of oversampling is more important at low SNR. For $S=1$ or 2 samples per symbol, the results obtained with the EKF are close to the theoretical bound for slow and moderate phase evolutions. For $S=4$, the HCRB is lower than for $S=2$ but the EKF performance does not show the same improvement. We also note the limitations of the algorithm when having an extremely rapidly varying phase evolution with respect to the symbol interval.

We have shown the good performance of the iterative block method proposed for joint time-delay and carrier estimation for high and moderate SNR, and an acceptable estimation performance in low SNR scenarios. This method is based on a two-step iterative method, including the oversampled carrier synchronization solution based on the EKF. The convergence of the method directly depends on the phase and Doppler distortion, and on the estimation of the carrier phase provided by the EKF stage. For a slowly varying carrier phase the algorithm convergence is really fast, and as the phase offset gets stronger the algorithm needs more iterations to converge to the good time-delay value.

Acknowledgement

This work has been partially supported by project 2009 SGR 1236 of the Catalan Administration (AGAUR), by LURGA project of the French ANR (Agence Nationale de la Recherche), by the Spanish Science and Technology Commission: TEC 2010-19171 (MOSAIC) and by the European Commission in the framework of the COST Action IC0803 (RFCSET).

References

[1] J. Vilà-Valls, J.-M. Brossier, L. Ros, On-line Hybrid Cramér–Rao Bound for Oversampled Dynamical Phase and Frequency Offset Estimation, IEEE Globecom 2009, Hawaii, 30 November–4 December 2009.
[2] B.W. Parkinson, J.J. Spilker, Global Positioning System: Theory and Applications, vol. 1, American Institute of Aeronautics and Astronautics, Washington, DC, 1996.
[3] European GNSS (Galileo)—Open Service. Signal In Space Interface Control Document. Ref.: OS SIS ICD, Issue 1.1, EU, September 2010.
[4] P.M. Woodward, Probability and Information Theory, with Application to Radar, Pergamon Press, New York, 1953.
[5] H.L. Van Trees, Detection, estimation, modulation theory, Part III: Radar–Sonar signal processing and Gaussian signals in noise in: Parameter Estimation: Slowly Fluctuating Point Targets, Wiley, 2001, pp. 275–356 (Chapter 10).
[6] E.D. Kaplan, C.J. Hegarty (Eds.), Understanding GPS. Principles and Applications, Mobile Communications Series, second ed.,Artech House, Norwood, MA, 2006.
[7] H. Meyr, M. Moeneclaey, S. Fetchel, Digital Communication Receivers: Synchronization, Channel Estimation and Signal Processing, Wiley, New York, 1998.

[8] U. Mengali, A.N. D'Andrea, Synchronization Techniques for Digital Receivers, Plenium Press, New York, 1997.
[9] M.P. Fitz, Planar filtered techniques for burst mode carrier synchronization, in: Proceedings of the IEEE GLOBECOM 1991, Phoenix, AZ, December 1991.
[10] B.D. O Anderson, J.B. Moore, Optimal Filtering, Prentice Hall, Englewood Cliffs, NJ, USA, 1979.
[11] P.J. Kootsookos, An extended Kalman filter for demodulation of polynomial phase signals, IEEE Signal Process. Lett. 5 (3) (1998).
[12] B.F. La Scala, R.R. Bitmead, Design of an extended Kalman filter frequency tracker, IEEE Signal Process. Lett. 5 (3) (1998).
[13] A. Aghamohammadi, H. Meyr, G. Ascheid, Adaptive synchronization and channel parameter estimation using an extended Kalman filter, IEEE Trans. Commun. 37 (11) (1989).
[14] L.-L. Cheng, Z.-G. Cao, GPS Carrier phase measurement method based on data transition detection in high dynamic circumstance, Proceedings of the WCC-ICCT, vol. 2, 21–25 August 2000.
[15] A.P. Dempster, N.M. Laird, D.B. Rubin, Maximum likelihood from incompleter data via EM algorithm, J. R. Statist. Soc. 39 (1) (1998).
[16] T.Y. Al-Naffouri, An EM-based forward-backward Kalman filter for the estimation of time-variant channels in OFDM, IEEE Trans. Signal Process. 55 (7) (2007) 3924–3930.
[17] T.Y. Al-Naffouri, A.A. Quadeer, A forward-backward Kalman filter-based STBC MIMO OFDM receiver, EURASIP J. Adv. Signal Process. 2008, January 2008.
[18] V. Digalakis, J. Rohlicek, M. Ostendorf, ML estimation of a stochastic linear system with the EM algorithm and its application to speech recognition, IEEE Trans. Speech Audio Process. 1 (4) (1993) 431–442.
[19] M.E. Khan, D.N. Dutt, An expectation-maximization algorithm based Kalman smoother approach for event-related desynchronization (ERD) estimation from EEG, IEEE Trans. Biomed. Eng. 54 (7) (2007) 1191–1198.
[20] H. Chen, R. Perry, K. Buckley, Direct and EM-based MAP sequence estimation with unknown time-varying channels, Proceedings of the IEEE International Conference on Acoustics, Speech, and Signal Processing, vol. 4, 2001, pp. 2129–2132.
[21] J.F.G. de Freitas, M. Niranjan, A.H. Gee, Nonlinear state space learning with EM and neural networks, in: IEEE International Workshop on Neural Networks in Signal Processing, Cambridge, England, 1998, pp. 254–263.
[22] H.L. Van Trees, Detection, Estimation and Modulation Theory, vol. 1, Wiley, New York, 1968.
[23] P. Tichavský, C.H. Muravchik, A. Nehorai, Posterior Cramér–Rao bounds for discrete-time nonlinear filtering, IEEE Trans. Signal Process. 46 (May) (1998) 1386–1396.
[24] S. Bay, B. Geller, A. Renaux, J.-P. Barbot, J.-M. Brossier, On the Hybrid Cramér–Rao bound and its application to dynamical phase estimation, IEEE Signal Process. Lett. 15 (2008) 453–456.
[25] J. Vilà-Valls, J.-M. Brossier, L. Ros, Oversampled phase tracking in digital communications with large excess bandwidth, Signal Process. 90 (3) (2010) 821–833.
[26] P.O. Amblard, J.-M. Brossier, E. Moisan, Phase tracking: what do we gain from optimality? Particle filtering versus phase-locked loops, Signal Process. 83 (October) (2003) 151–167.
[27] S. Bay, C. Herzet, J.-M. Brossier, J.-P. Barbot, B. Geller, Analytic and asymptotic analysis of Bayesian Cramér–Rao bound for dynamical phase offset estimation, IEEE Trans. Signal Process. 56 (January) (2008) 61–70.
[28] B.D. O Anderson, J.B. Moore, Optimal Filtering, Prentice Hall, Englewood Cliffs, NJ, USA, 1979.